Sampling-Oscilloscope Measurement of a Microwave Mixer With Single-Digit Phase Accuracy

Dylan F. Williams, *Fellow, IEEE*, Hassen Khenissi, Fabien Ndagijimana, Kate A. Remley, *Member, IEEE*, Joel P. Dunsmore, *Member, IEEE*, Paul D. Hale, *Senior Member, IEEE*, Jack C. M. Wang, and Tracy S. Clement, *Senior Member, IEEE*

***Abstract*—We describe a straightforward method of separately characterizing up- and down-conversion in microwave mixers using a sampling oscilloscope. The method mismatch-corrects the results, determines both magnitude and phase, and uses a novel time-base correction scheme to improve the accuracy of the measurements. We estimate our measurement accuracy to be on the order of a tenth of a decibel in magnitude and a few degrees in phase. We use the method to characterize the magnitude and phase reciprocity of a microwave mixer.**

***Index Terms*—Down-conversion, frequency translation, jitter correction, magnitude measurement, mismatch correction, mixer measurement, mixer reciprocity, oscilloscope, phase measurement, time-base correction, up-conversion.**

I. Introduction

We demonstrate separate mismatch-corrected measurements of the magnitude and phase of a microwave mixer's up- and down-conversion transfer functions. The method uses a conventional sampling oscilloscope to measure the input and output signals of the mixer, and a vector network analyzer (VNA) to perform measurements required for the mismatch corrections. We also employ a novel measurement setup and algorithm to correct for jitter, drift, and distortion in the oscilloscope's time base. The resulting measurements are accurate enough to characterize "golden" diode-based reference mixers suitable for use with multifrequency VNAs equipped for mixer characterization.

Microwave mixer measurements are, in general, quite complicated because the input and output frequencies of the mixers are different. In addition, Torrey and Whitmer observed in 1948 that mixers are not, in general, reciprocal [1], i.e., the up- and down-conversion transfer functions of even diode-based mixers are not generally equal. Thus, a complete characterization of a microwave mixer requires that the up- and down-conversion transfer functions be measured separately [1], [2].

It is possible to use a single-frequency VNA to measure the "round-trip" product of the up- and down-conversion transfer functions of a mixer using deembedding methods [3]–[5]. These approaches are based on measuring the input impedance of the mixer at its input port while connecting a number of known impedances to the output port of the mixer.

These methods are similar to deembedding methods used to characterize electrical adapters and transitions at microwave frequencies [6], and are easy to perform because the VNA impedance measurements need be performed at only a single frequency at the input port of the mixer. However, these methods measure the mean of the mixer's up- and down-conversion transfer functions, and cannot distinguish differences between them. This is because the transfer function of the mixer is measured by signals that first go forward through the mixer, are then reflected off the load connected to the mixer's output port, and finally traverse backward through the mixer again,

The magnitude of the up- and down-conversion loss of a mixer can be measured directly with a VNA and supplementary power calibration, as described in [3] or [7]. However, this "power-meter-calibrated" VNA approach does not measure the phase of the mixer transfer function. Thus, separately characterizing the phase response of a mixer is still the most difficult aspect of its characterization, and characterizing the difference in the phase of the up- and down-converted signals of microwave mixers, and particularly of diode-based reference mixers, remains problematic.

Reference mixers are often characterized with the "three-mixer method." This method is based on VNA measurements of the product of signals up-converted by one mixer and down-converted by another. These measurements are fairly straightforward, as the frequencies of the incident and reflected signal at the mixer port are the same. When three mixers are measured in various combinations [8]–[12], it is possible to uniquely determine the separate up- and down-conversion transfer functions of all three mixers if one of the three mixers is reciprocal. However, this still leaves open the question of how one determines that the phase response of one of the three mixers is reciprocal.

Van Moer and Rolain suggested an approach for separately measuring the phase of the up- and down-conversion transfer functions of microwave mixers with a three-port large-signal network analyzer (LSNA) in [13]. The LSNA separately measures the signals at all three ports of the mixer, and is thus able to measure both the magnitude and phase of the up- and down-conversion transfer functions separately. While this method is extremely precise, it requires custom instrumentation and lacks the frequency resolution to adequately characterize a mixer's phase reciprocity in the conventional way. In [13], the authors did not

Manuscript received September 17, 2005.

D. F. Williams, K. A. Remley, P. D. Hale, J. C. M. Wang, and T. S. Clement are with the National Institute of Standards and Technology, Boulder, CO 80305 USA (e-mail: dylan@boulder.nist.gov).

H. Khenissi was with the Université Joseph Fourier, 38041 Grenoble, France.

F. Ndagijimana is with the Université Joseph Fourier, 38041 Grenoble, France and also with the Institut Universitaire de Technologie de Grenoble, 38031 Grenoble, France.

J. P. Dunsmore is with Agilent Technologies, Santa Rosa, CA 95404 USA.

Digital Object Identifier 10.1109/TMTT.2005.864102

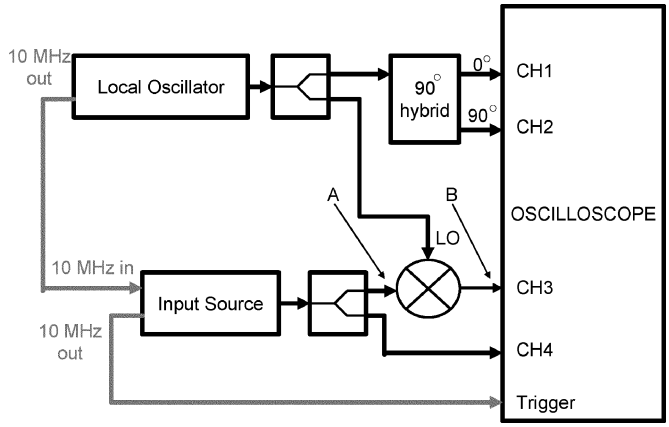

Fig. 1. Our measurement setup. Not shown in this figure are an isolator in the LO path and 16-dB attenuators at the two output ports of the lower splitter that prevent signals reflected from or generated in the mixer from interfering with the signals on channels 1, 2, and 4.

account for the effect of the local-oscillator phase in the conventional way, resulting in apparent nonreciprocal behavior.

Boulejfen *et al.* [14] suggest a similar approach that overcomes the frequency restrictions of [13]. However, their approach is based on a custom setup requiring a number of couplers, switches, a microwave transition analyzer, and other components.

Nevertheless, microwave mixers are most commonly characterized with a VNA and a diode reference mixer whose up- and down-conversion transfer functions have already been determined by other means [8]–[12]. Typically, the methods of characterizing the reference mixer assume phase reciprocity.

Here, we develop a measurement approach based on widely available sampling oscilloscopes for characterizing microwave mixers. The procedure separately measures both the magnitude and phase of the up- and down-conversion transfer functions of a microwave mixer on a nearly arbitrary frequency grid. The approach is accurate and greatly simplifies the characterization of reference mixers for VNA calibrations.

II. Measurement System

We use a four-channel oscilloscope and the setup shown in Fig. 1 to measure the two transfer functions of microwave mixers. We first characterize the signal from the source at the input of the mixer by connecting the source output at A to channel three of the oscilloscope. This requires removing the mixer from the setup and inserting an adapter in its place. During the source characterization, we also measure the reference signal on channel 4. This reference signal helps us to later reconstruct the actual magnitude and phase of the signal at A when the mixer is being tested.

After characterizing the relationships between the source signal at A and the signal measured on channel 4 of the oscilloscope, we insert the mixer as shown in the figure. We then measure the signal at B at the output of the mixer on channel 3 of the oscilloscope. Since we are able to determine the magnitude and phase of the signal at the mixer's input port at A from our measurement on channel 4, after correcting for mismatch, we can directly calculate the difference in the magnitude and phase between the input and output signals of the mixer and, thus, determine its transfer function in the setup.

During all of the measurements, we simultaneously measure "copies" of the local oscillator and source signals on channels 1, 2, and 4 of the oscilloscope to correct for drift and jitter in the oscilloscope time base, as described below. This allows us to set the time reference for our measurements to a constant phase of the local oscillator, and to better determine the relative phases of all of the signals in the experiment in the presence of drift and jitter in the reference signals that lock the sources together and trigger the oscilloscope, and in the presence of distortion in the oscilloscope time base.

A. Time Base

To establish a uniform time base for the sources and oscilloscope, we lock the local oscillator and input sources together and trigger the oscilloscope with the 10-MHz reference signals shown in Fig. 1. If there were no jitter or drift in these 10-MHz locking and trigger circuits relative to the microwave sources and oscilloscope trigger, and if there were no distortion in the oscilloscope time base, we would only need the measurements of the signals at A and B in this figure to accurately measure the transfer functions of the mixer. Unfortunately, there is a great deal of jitter and drift in the 10-MHz locking circuits, and the distortion in the oscilloscope time base is not negligible.

We surmount these problems by adding the splitters and hybrid couplers shown in Fig. 1 to the measurement setup. These splitters and couplers allow us to measure copies of the signals from the source and local oscillator simultaneously with the measurements we perform on channel 3. The supplementary measurements on channels 1, 2, and 4 of the oscilloscope allow us to correct the time-base distortion in the oscilloscope, and to track and correct for the jitter and drift in the 10-MHz locking and trigger circuits.

The procedure that we use to correct for jitter, drift, and time-base distortion is described in [15], and is based on the fact that, in our oscilloscope, a single strobe is used to close the four sampling gates. Since the same strobe pulse is split and used to close the sampling gates of the oscilloscope, the voltage samples on each channel of the oscilloscope are taken at nearly the same time, i.e., the relative times between when the samples are taken on each channel are almost impervious to the much larger jitter and drift in the oscilloscope time base, and remain very nearly the same even in the presence of large overall drift and jitter.

The new time base for the measurements is based on first fitting distorted sine waves to the copies of the local-oscillator signals we measure on channels 1 and 2 of the oscilloscope [15]. These signals are indicated by thin black lines in Fig. 2. During the actual adapter and mixer measurements, we then use the algorithm described in [15] as implemented in the freeware package [16] to adjust our estimates of the time that the oscilloscope actually performed its measurement. This is achieved by finding the measurement time for each sample that best aligns the voltages measured on channels 1 and 2 of the oscilloscope with our distorted sine-wave fits. Since all four samplers in the oscilloscope are driven by the same strobe pulse, this procedure results in an extremely precise determination of the measurement time with respect to the local-oscillator signals, and eliminates distortion in the oscilloscope time base [15].

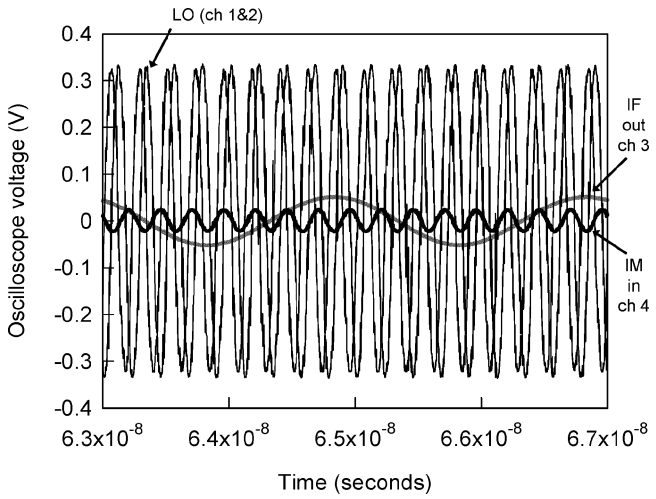

Fig. 2. Typical oscilloscope traces measured during our experiment before time-base and jitter correction. The thin traces are the in-phase and quadrature copies of the local oscillator measured on channels 1 and 2 of the oscilloscope. These traces are used to establish the time base. The thick black line is the copy of the signal going into the image port of the mixer measured on channel 4 of the oscilloscope. The thick grey line is the signal at the IF output of the mixer measured on channel 3 of the oscilloscope.

An important advantage of our new time base is that the measurement time is determined in terms of the in-phase and quadrature copies of the local-oscillator signals we measure on channels 1 and 2. This is extremely convenient, as we are able to perform all of our measurements with respect to a fixed local-oscillator phase even as the input source and oscilloscope timebases drift with respect to the local oscillator.

B. Source Characterization

After establishing our time base for the measurements with the local-oscillator signals, we characterize the source (labeled "input source" in Fig. 1). We do this by placing an adapter in the setup where the mixer is shown in Fig. 1, and use channel 3 of the oscilloscope to measure the signal at the point marked "B" just after the adapter. We then determine the magnitude and phase of the signal we are interested in by fitting a sine wave to the temporal signal measured by the oscilloscope. Finally, using a VNA measurement of the scattering parameters of the adapter and the reflection coefficients of the source and oscilloscope, we deembed the measurement and determine the magnitude and phase of the signal emanating from the source at reference plane A.

During this source characterization step, we simultaneously measure the copy of the source signal on channel 4 of the oscilloscope, and determine its magnitude and phase by fitting to a sine wave. This allows us to determine the relationship between the magnitude and phase of the source signal at A and the magnitude and phase of the signal measured on channel 4 of the oscilloscope. Later we determine the magnitude and phase of the input signal at A in Fig. 1 from our measurements on channel 4 of the oscilloscope during the actual mixer tests. To ensure fixed relationships between the signal measured on channel 4 and the signal at A, we inserted two 16-dB attenuators (not shown in Fig. 1) on the two output ports of the lower splitter in this figure to prevent signals reflected by the mixer or oscilloscope port 3 from reflecting back and being measured on channel 4 of the oscilloscope.

C. Mixer Characterization

Next we characterize the mixer itself. We begin by removing the adapter and inserting the mixer in its place. During this phase of the measurement procedure, the setup is as shown in Fig. 1. We measure the up-converted signal at the point marked "B" in this figure emanating from the mixer on channel 3 of the oscilloscope, as well as the copies of the source and local-oscillator signals discussed above on the other channels of the oscilloscope. Fig. 2 plots typical signals we measure on the four channels of the oscilloscope.

Next we calculate the actual source voltage $v_{\rm s}$ at point A in Fig. 1 from the reference voltage $v_{\rm r}$ measured on channel 4 of the oscilloscope with $v_{\rm s} = v_{\rm s1}(v_{\rm r}/v_{\rm r1})$, where $v_{\rm s1}$ is the voltage of the source we characterized with the adapter in place, and $v_{\rm r1}$ was the voltage we measured on channel 4 of the oscilloscope when we characterized the source voltage $v_{\rm s1}$. Again, we use sine-wave fits to determine the magnitudes and phases of these voltages.

Finally, we reverse the direction of the mixer and measure the down-converted signal emanating from the mixer at B. Again, we use our measurement on channel 4 to compensate for drift in the measurement setup. A comparison of the magnitude and phase of these signals allows us to determine the magnitude and phase of the up- and down-conversion transfer functions of the mixer.

D. Transformation to a Single-Frequency Problem

Once we have determined the magnitude and phase of the signals at the input A to the mixer and the output B of the mixer, we are ready to account for all of the mismatches in the measurement system, and to solve for the mixer transfer functions. We begin this correction process by measuring the reflection coefficients of the mixer with a VNA using the method of [3]. This is a straightforward process since it involves measuring only single-frequency reflection coefficients of the mixer with various loads terminating the other port of the mixer.

These measurements, when combined with the reflection coefficient of the oscilloscope on channel 3 we measured previously at point B in Fig. 1 and the source impedance we measured previously at point A in Fig. 1, leaves us with only two unknowns in the measurements, i.e., the up- and down-conversion transfer functions of the mixer. We determined these two unknown transfer functions by iteratively adjusting them until the up- and down-converted voltages we calculated from an equivalent-circuit model of our measurement setup agree with the up- and down-converted voltages we measured on channel 3 of the oscilloscope.

We used the mixer representations and procedures described in [17] to transform the multifrequency setup of Fig. 1 to a single-frequency problem. While, as explained in [17], this requires some bookkeeping to properly match up the different frequencies in the problem, it greatly simplifies the models and the calculations. Following [17], we represented our mixer, which is surrounded by the dashed boxes in the equivalent circuits of Figs. 3 and 4, with a scattering parameter "error box" and an ideal mixer. The ideal mixer has an unknown, but constant local-oscillator phase represented by the phase of $a_{\rm LO}$, where $|a_{\rm LO}| = 1$.

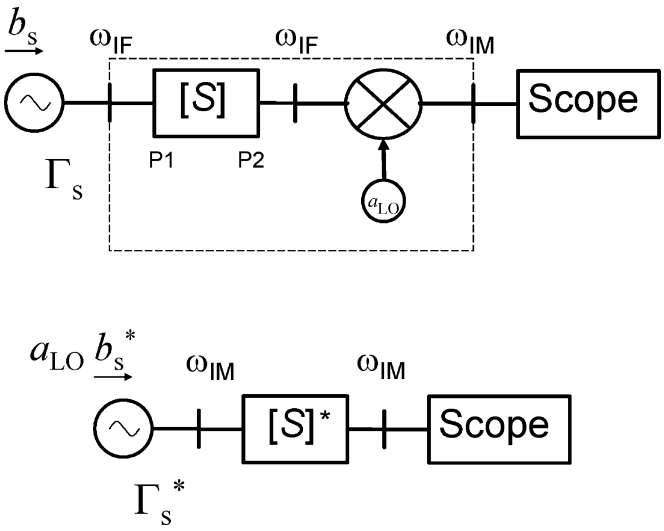

Fig. 3. Reduction of the multifrequency up-conversion measurement problem to a single-frequency equivalent circuit. The ideal mixer conjugates $[S]$, b_s, and Γ_s as it is moved to the left and combined with the source using the rules outlined in [17].

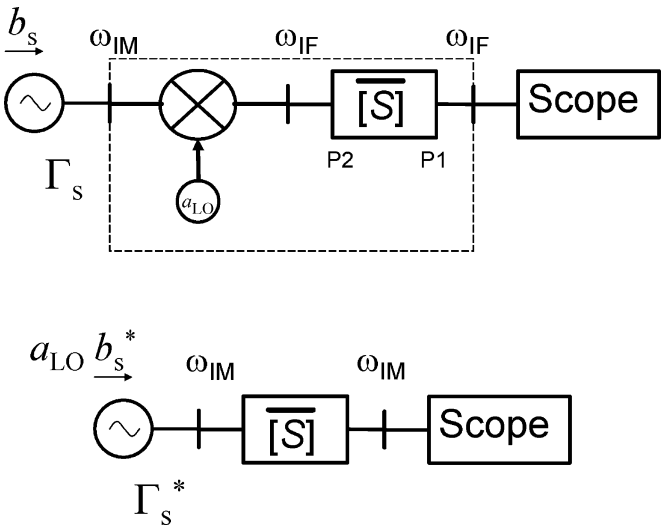

Fig. 4. Reduction of the multifrequency down-conversion measurement problem to a single-frequency equivalent circuit. The ideal mixer conjugates only b_s and Γ_s as it is combined with the source using the rules outlined in [17].

In our experiments, we used an image mixer. Figs. 3 and 4 illustrate the procedure for an image mixer: similar procedures for an RF mixer are presented in [17].

The equivalent circuits in Fig. 3 correspond to the up-conversion measurement. The sketch at the top of this figure shows the actual multifrequency circuit, and the sketch at the bottom of this figure shows the single-frequency equivalent circuit after the ideal mixer in the circuit at the top of this figure has been "moved through" the scattering-parameter error box $[S]$ describing the nonideal behavior of the mixer and the source, as described in [17].

Note that, as the ideal image mixer is moved through scattering-parameter error boxes and combined with sources following the rules outlined in [17], it not only translates the frequency of the measurements, but conjugates the phase of the elements describing these error boxes and sources. This conjugation behavior is due to the phase reversals that take place in image mixing, and do not occur for regular RF mixers [17].

The equivalent circuits in Fig. 4 correspond to the down-conversion measurement. The bar over the scattering-parameter error box indicates that the error box in Fig. 4 points in the opposite direction: i.e., $\overline{S}_{11} \equiv \overline{S}_{22}$, $\overline{S}_{21} \equiv \overline{S}_{12}$, $\overline{S}_{12} \equiv S_{21}$, and $\overline{S}_{22} \equiv S_{11}$. Again, as the ideal image mixer is moved through scattering-parameter error boxes and combined with sources, it conjugates the phase of the elements describing these error boxes and sources.

E. Iterative Solution Procedure

Finally, we used our single-frequency equivalent-circuit models describing the measurement setup to numerically solve for the transfer functions $a_{\rm LO}S_{12}$ and $a_{\rm LO}S_{21}^*$ of the mixer from the measurements. Recall that we already measured the reflection coefficients S_{11} and S_{22} of the mixer, source, and oscilloscope with our VNA, leaving as unknowns only $a_{\rm LO}S_{12}$ and $a_{\rm LO}S_{21}^*$ in the equivalent circuits of Figs. 3 and 4.

To solve for these transfer functions, we began with a guess of 1 for $a_{\rm LO}S_{12}$ and $a_{\rm LO}S_{21}^*$, and iteratively adjusted them until the calculated magnitude and phase of the signal at the output of our mixer (point B in Fig. 1) in our equivalent-circuit model matched the actual magnitude and phase measured by the oscilloscope on channel 3. The solutions are easy to find as the ratio of the measured input and output signals in our setup are very nearly given by the terms $a_{\rm LO}S_{12}$ and $a_{\rm LO}S_{21}^*$, and the reflection coefficients only perturb the measurements slightly. This makes the solution algorithm very nearly linear and, as a result, there are no local minima to complicate finding the solution.

We were able to greatly speed this procedure by estimating new values $(a_{\rm LO}S_{12})_{\rm new}$ and $(a_{\rm LO}S_{21}^*)_{\rm new}$ for $a_{\rm LO}S_{12}$ and $a_{\rm LO}S_{21}^*$ from the current guesses $(a_{\rm LO}S_{12})_{\rm guess}$ and $(a_{\rm LO}S_{21}^*)_{\rm guess}$ for $a_{\rm LO}S_{12}$ and $a_{\rm LO}S_{21}^*$. We used the formula $(a_{\rm LO}S_{12})_{\rm new} = (a_{\rm LO}S_{12})_{\rm guess}(v_{\rm meas}/v_{\rm calc})$ to update our guess for $a_{\rm LO}S_{12}$, where $v_{\rm meas}$ is the voltage of the source we measured on channel 3 of the oscilloscope, and $v_{\rm calc}$ is the voltage we calculated that we should have measured on channel 3 of the oscilloscope from the measured reflection coefficients and estimates $(a_{\rm LO}S_{12})_{\rm guess}$ and $(a_{\rm LO}S_{21}^*)_{\rm guess}$. Likewise, we used the formula $(a_{\rm LO}S_{21}^*)_{\rm new} = (a_{\rm LO}S_{21}^*)_{\rm guess}(v_{\rm meas1}/v_{\rm calc1})$ at each iteration step to update our guess for $a_{\rm LO}S_{21}^*$, where $v_{\rm meas1}$ is the voltage of the source we measured on channel 3 of the oscilloscope, and $v_{\rm calc1}$ is the voltage we calculated that we should have measured on channel 3 of the oscilloscope from the measured reflection coefficients and estimates $(a_{\rm LO}S_{12})_{\rm guess}$ and $(a_{\rm LO}S_{21}^*)_{\rm guess}$ when the mixer was reversed.

Our iterative procedure was extremely fast and robust, and we were able to achieve convergence of one part in 10^{-10} in only six or seven iterations. In practice, we found that it not worth implementing and checking stopping conditions, as simply performing ten iterations of the algorithm achieves convergence to better than one part in 10^{-10}.

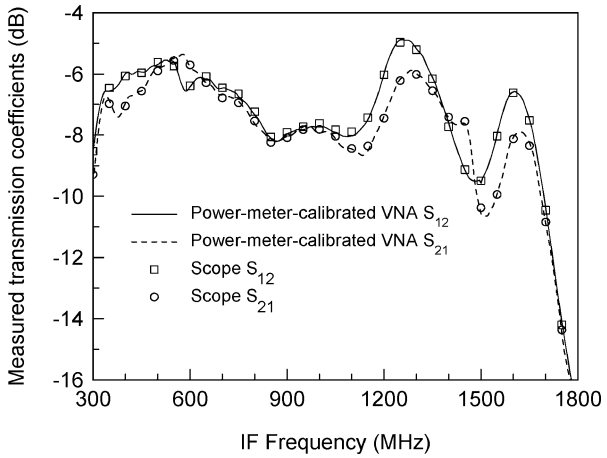

Fig. 5. Comparison of the up-conversion loss $|S_{21}|$ and down-conversion loss $|S_{12}|$ measured with our oscilloscope and a power-meter-calibrated VNA.

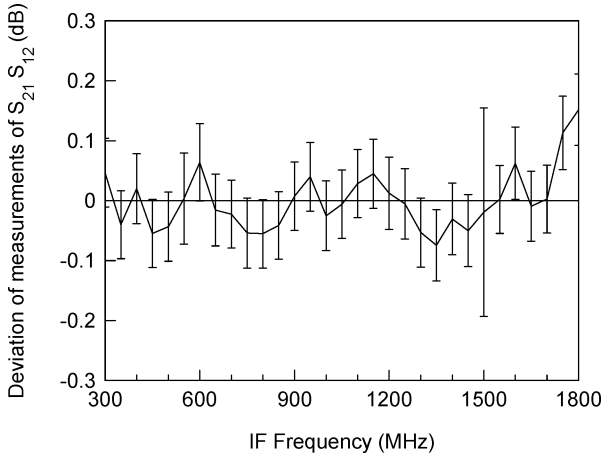

Fig. 6. Comparison of the product of the up- and down-conversion loss $|S_{21}\ S_{21}|$ measured with our oscilloscope and the average of the round-trip conversion losses measured with a VNA.

III. Measurement Results

We used a commercial off-the-shelf 2000–4200-MHz balanced diode mixer at a local-oscillator frequency of 4500 MHz to demonstrate our measurement system. We arranged the mixer in an image configuration, and added a low-pass filter with a cutoff frequency of 1650 MHz to the IF port, and a 2000–4000-MHz bandpass filter on the image port. These filters reduced local-oscillator leakage to the other ports, and suppressed other mixing products at the mixer's IF and image ports. These filters reduce the sensitivity of the mixer to terminations at the local-oscillator frequency and higher order mixing products, and ensure validity of the assumptions of [17].

We also added dc blocking capacitors to the mixer's intermediate and local-oscillator ports, and the bandpass filter on the image port served as a dc block on that port as well. These dc blocks eliminated any sensitivity of the mixer to dc bias and the dc return paths applied to the mixer. Finally, we tested our image mixer, which consisted of the diode mixer, filters, and dc blocks, on our measurement system. We then measured the transfer function of the mixer plus filters and dc blocks, which we simply refer to as our mixer in what follows.

Fig. 5 compares the mixer's up-conversion loss $|S_{21}|$ and down-conversion loss $|S_{12}|$ we measured with our oscilloscope to the same quantities measured by a power-meter-calibrated VNA [3], [7]. This figure shows excellent agreement between the measurements.

Fig. 6 plots the difference of the product $|S_{21}S_{12}|$ and the average of two round-trip measurements of that same quantity measured with our VNA, using the method of [4]. Again, the agreement is excellent.

The error bars in Fig. 6 represent our estimate of the standard uncertainty in the measurements. Table I summarizes the different components of these uncertainty estimates. We estimated the standard uncertainty due to repeatability in our measurements from three repeat measurements of the mixer. To this we added estimates of our uncertainty in the swept-sine magnitude corrections for our oscilloscope response, which we performed following the procedure described in [18], and combined our uncertainties following the recommendations of [19]. As can be seen in this table, the systematic part of our estimated uncertainties dominated the total uncertainty.

TABLE I
Estimated Standard Uncertainties for Measurements of the Mixer's Transfer Function

Error Source	Magnitude (dB)	Phase (degrees)	Degrees of freedom [19]
Repeatability (typical)	0.015	0.205	2
Oscilloscope magnitude calibration	0.04	–	∞
Deviation from EOS-calibrated measurements	–	1.235	∞
Input cable	–	0.043	∞
LO cable	–	0.217	∞
Total std. uncert. (typical)	0.043	1.274	> 1000

As we do not possess accurate low-frequency electrical phase standards, we were not able to calibrate the oscilloscope's phase response. We set the systematic phase uncertainty equal to the standard deviation of the differences of oscilloscope measurements of a photodiode to calibrated phase measurements of the same photodiode performed on the National Institute of Standards and Technology (NIST) electrooptic sampling system described in [20]. We believe that these differences were, for the most part, due to errors in the electrooptic sampling system, which is designed primarily for high-frequency measurements [21], and not to the oscilloscope's phase response. Thus, our actual phase measurement errors could be significantly smaller than our uncertainty estimates.

IV. Phase and Phase Reciprocity

As discussed earlier, we used our time-base correction algorithm to hold the phase of the local-oscillator drive term a_{LO} constant during the measurements. Thus, our measurements of the signal at the input to the oscilloscope at B in these

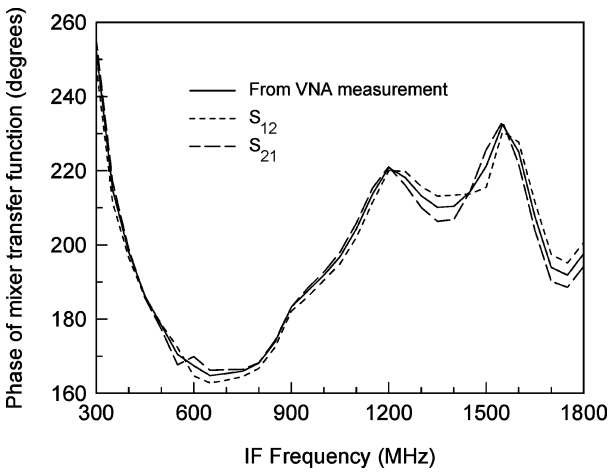

Fig. 7. Comparison of the phases of S_{21} and S_{12} measured with our oscilloscope and with the average round-trip phase measured with our VNA. We subtracted a constant offset to account for the unknown phase of $a_{\rm LO}$ and a constant delay to better show the mixer's phase distortion.

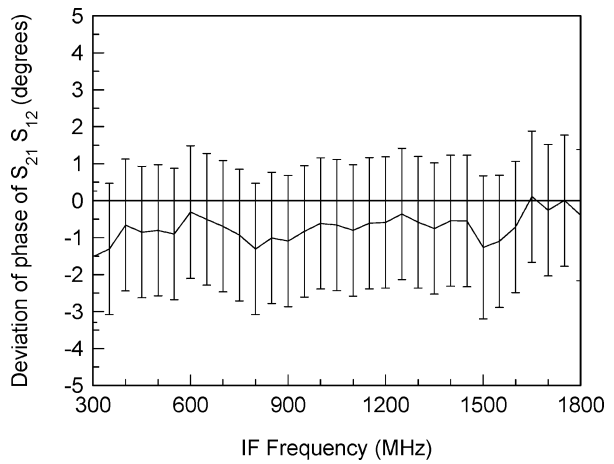

Fig. 8. Comparison of the phase of the product $S_{21}\ S_{12}$ measured with our oscilloscope and with a VNA.

figures allow us to measure the two transfer functions $a_{\rm LO}S_{12}$ and $a_{\rm LO}S_{21}^*$, as is clear from the single-frequency equivalent circuits at the bottom of Figs. 3 and 4. Fig. 7 compares the phase of S_{21} and S_{12} of our mixer after subtracting a constant due to the phase of $a_{\rm LO}$, and after subtracting a constant delay. Not only does this figure shows good agreement with the round-trip VNA measurement based on the method of [4], it shows that the phase response of the mixer is, for the most part, reciprocal.

Fig. 8 plots the difference between the phase of the product $S_{21}S_{12}$ and the average of the two round-trip measurements of that same quantity measured with our VNA using the method of [4]. In this case, the measurements agree to within approximately a degree, illustrating the high accuracy achievable with the sampling oscilloscope.

Fig. 8 also shows that our oscilloscope phase measurements agree with our round-trip VNA measurements to well within our estimated uncertainties. Like our random magnitude uncertainty estimates, we derived our random phase uncertainty from three

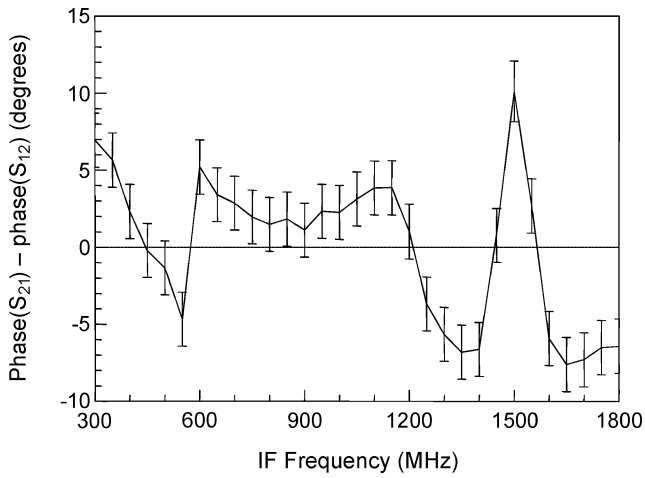

Fig. 9. Difference of the phase of S_{21} and S_{12} measured with our oscilloscope after subtracting a constant offset due to the unknown phase of the local oscillator.

repeated measurements, and the systematic uncertainties in the phase from a comparison to measurements we performed on the NIST electrooptic sampling system. To these, we added smaller uncertainties due to cable bending during the measurements, which we also characterized with our VNA.

As we pointed out in Section I, mixer reciprocity, and particularly mixer phase reciprocity, has been a troublesome issue since World War II. Our oscilloscope measurement method addresses the measurement of mixer phase reciprocity directly.

The unknown phase of the local oscillator in the models of Figs. 3 and 4 results in an absolute phase offset in the measured transfer functions $a_{\rm LO}S_{12}$ and $a_{\rm LO}S_{21}^*$.[1] Fig. 9 plots the phase of $a_{\rm LO}^2S_{12}/S_{21}$ we measured after subtracting the constant offset in this quantity. This is, to within a constant offset, the difference in the phases of S_{12} and S_{21}.

We were surprised by the fairly large and rapid changes in the difference of the phases of S_{12} and S_{21}, particularly between 550–600 MHz, where the amplitude response of the mixer is fairly smooth. We can only speculate at this point that this difference in phase near 600 MHz is related to the small dip in the magnitude of S_{12}, shown in Fig. 5, and that this sharp phase change is related to some resonance in the reflective filters that we used in our mixer. While we did not perform measurements over a fine enough frequency grid to accurately determine the differences in the up- and down-conversion group delay of our mixer, the measurements do indicate differences in the up- and down-conversion group delay of at least 0.5 ns.

[1]While we could have measured the phase of the local-oscillator signal at the local-oscillator port of the mixer in our experiments, there would still have been a constant, but unknown phase difference between the phase of $a_{\rm LO}$ at the physical local-oscillator input of the mixer and phase of $a_{\rm LO}$ at the ideal mixer in the equivalent-circuit models of Figs. 2 and 3 [17]. Thus, we can never determine the absolute difference of the phases of S_{21} and S_{12} from the two measured transfer functions $a_{\rm LO}S_{12}$ and $a_{\rm LO}S_{21}^*$.

In most applications, the phase of $a_{\rm LO}$ is not controlled, and the absolute offsets of the phases of S_{21} and S_{12} introduced by the phases of the local-oscillator frequency are unimportant. Rather, the most important information about mixer behavior from a system point-of-view is contained in the way that S_{21} and S_{12} evolve with frequency. This explains the focus on the measurement of the group delay of mixer transfer functions in the literature.

V. Conclusion

The method we presented here measures the magnitude and phase reciprocity of microwave mixers with relatively inexpensive instrumentation. We showed that our measurement scheme is quite accurate, and easily able to distinguish differences in the evolution of the phases of the transfer functions of microwave mixers with frequency that are ignored by the VNA deembedding method of [3] and [4]. Measuring these phase differences with the methods of [8], [9], [22], and [23] would require a calibrated reference mixer. Only the method described in [14] could have measured this phase difference on a frequency grid fine enough to determine group delay, but requires significantly greater resources to perform.

The frequencies we used were low enough that it was not necessary to correct for the phase response of our oscilloscope. However, as the frequency of the local oscillator increases, so does the slope of the sinusoids. The increase in the slope of the sinusoids improves our ability to determine at what time our measurements were performed in the presence of additive noise from the voltages measured on channels 1 and 2 of the oscilloscope. Thus, our approach to establishing a uniform time base for the measurements scales well to higher frequencies. Furthermore, we could also measure and correct for the oscilloscope phase response at higher frequencies with a photodiode characterized on our electrooptic sampling system.

While here we described only experiments employing small-signal sinusoidal excitation, the apparatus can also be used to characterize more complex mixer behavior with large-signal multitone excitations. We could have equally well applied the approach to the characterization of highly nonreciprocal active transistor mixers.

References

[1] H. C. Torrey and C. A. Whitmer, *Crystal Rectifiers*. New York: McGraw-Hill, 1948.

[2] S. Maas, *Microwave Mixers*. Boston, MA: Artech House, 1992.

[3] J. Dunsmore, "Novel method for vector mixer characterization and mixer test system vector error correction," in *IEEE MTT-S Int. Microwave Symp. Dig.*, vol. 3, Jun. 2002, pp. 1833–1836.

[4] J. Dunsmore, S. Hubert, and D. F. Williams, "Vector mixer characterization for high-side LO cases," in *IEEE MTT-S Int. Microw. Symp. Dig.*, vol. 3, Jun. 2004, pp. 1743–1746.

[5] M. E. Knox, "A novel technique for characterizing the absolute group delay and delay linearity of frequency translation devices," in *ARFTG Conf. Dig.*, vol. 53, Jun. 1999, pp. 50–56.

[6] R. F. Bauer and P. Penfield, "De-embedding and unterminating," *IEEE Trans. Microw. Theory Tech.*, vol. MTT-22, no. 3, pp. 282–288, Mar. 1974.

[7] B. Roth, D. Kother, M. Coady, T. Sporkmann, and C. Sattler, "Applying a conventional VNA to nonlinear measurements without using frequency converting standards," in *3rd Int. Integr. Nonlinear Microw. Millimeterw. Circuits Workshop*, May 1994, pp. 243–252.

[8] C. J. Clark, A. A. Moulthrop, M. S. Muha, and C. P. Silva, "Transmission response measurements of frequency translating devices," in *IEEE MTT-S Int. Microw. Symp. Dig.*, vol. 3, Jun. 1996, pp. 1285–1288.

[9] ——, "Transmission response measurements of frequency-translating devices using a vector network analyzer," *IEEE Trans. Microw. Theory Tech.*, vol. 44, no. 12, pp. 2724–2737, Dec. 1996.

[10] ——, "Network analyzer measurements of frequency translating devices," *Microwave J.*, vol. 39, no. 11, pp. 114–126, Nov. 1996.

[11] D. R. Thornton, "A simple VNA method for mixer conversion loss measurement," *Microw. J.*, vol. 40, no. 3, pp. 78–86, Mar. 1997.

[12] M. L. Truong, "Increased accuracy of absolute group delay measurements," *Microw. J.*, vol. 42, no. 9, pp. 150–160, Sep. 1999.

[13] W. Van Moer and Y. Rolain, "Proving the usefulness of a 3-port nonlinear vectorial network analyzer through mixer measurements," in *IEEE MTT-S Int. Microw. Symp. Dig.*, vol. 3, Jun. 2003, pp. 1647–1650.

[14] N. Boulejfen, F. M. Ghannouchi, and A. B. Kouki, "A novel measurement technique for microwave frequency translating devices (FTD)," in *Precision Electromagn. Meas. Dig. Conf.*, Jul. 1998, pp. 422–423.

[15] P. D. Hale, C. M. Wang, D. F. Williams, K. A. Remley, and J. Wepman, "Compensation of random and systematic timing errors in sampling oscilloscopes," *IEEE Trans. Instrum. Meas.*, submitted for publication.

[16] P. D. Hale, C. M. Wang, D. F. Williams, K. A. Remley, and J. Wepman, "Time base correction (TBC) software package," NIST, Boulder, CO, 2005. [Online]. Available: http://www.boulder.nist.gov/div815/HSM_Project/Software.htm.

[17] D. F. Williams, F. Ndagijimana, K. A. Remley, J. Dunsmore, and S. Hubert, "Scattering-parameter models and representations for microwave mixers," *IEEE Trans. Microw. Theory Tech.*, vol. 53, no. 1, pp. 314–321, Jan. 2005.

[18] D. C. DeGroot, P. D. Hale, M. Vanden Bossche, F. Verbeyst, and J. Verspecht, "Analysis of interconnection networks and mismatch in the nose-to-nose calibration," in *Automatic RF Tech. Group Conf. Dig.*, vol. 55, Jun. 2000, pp. 116–121.

[19] B. N. Taylor and C. E. Kuyatt, "Guidelines for evaluating and expressing the uncertainty of NIST measurement results," NIST, Boulder, CO, Tech. Note 1297, Sep. 1994.

[20] T. S. Clement, P. D. Hale, D. F. Williams, and J. M. Morgan, "Calibrating photoreciever response to 110 GHz," in *15th Annu. IEEE Lasers and Electro-Opt. Soc. Meeting Conf. Dig.*, Nov. 2002, pp. 877–878.

[21] D. F. Williams, P. D. Hale, T. S. Clement, and C. M. Wang, "Uncertainty of the NIST electrooptic sampling system," NIST, Boulder, CO, Tech. Note 1535, Dec. 2004.

[22] "Amplitude and phase measurements of frequency translating devices using the HP 8510B network analyzer," Hewlett-Packard Company, Palo Alto, CA, Product Note 8510-7, 1987.

[23] D. Ballo, "Measuring absolute group delay of multistage converters," in *33rd Eur. Microw. Conf.*, vol. 1, Oct. 2003, pp. 89–92.

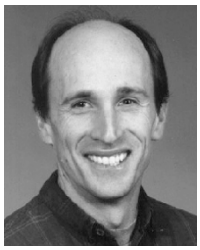

Dylan F. Williams (M'80–SM'90–F'02) received the Ph.D. degree in electrical engineering from the University of California at Berkeley, in 1986.

In 1989, he joined the Electromagnetic Fields Division, National Institute of Standards and Technology, Boulder, CO, where he develops metrology for the characterization of monolithic microwave integrated circuits and electronic interconnects. He has authored or coauthored over 80 technical papers.

Dr. Williams is an associate editor for the IEEE TRANSACTIONS ON MICROWAVE THEORY AND TECHNIQUES. He was the recipient of the Department of Commerce Bronze and Silver Medals, two Electrical Engineering Laboratory's Outstanding Paper Awards, two Automatic RF Techniques Group (ARFTG) Best Paper Awards, the ARFTG Automated Measurements Technology Award, and the IEEE Morris E. Leeds Award.

Hassen Khenissi received the Engineering degree (with a specialization in microelectronics and radio frequencies) from the Ecole Nationale Supérieure d'électronique et de Radioélectricité de Grenoble (ENSERG), Grenoble, France, in 2004, and the Master degree in opto-electronics and microwaves from the Institut National Polythecnique de Grenoble, Grenoble, France, in 2004.

He then joined the National Institute of Standards and Technology (NIST), Boulder, CO, for five months in 2004, where he was a Guest Researcher involved with the mixer characterization method using a calibrated oscilloscope.

Fabien Ndagijimana received the Ph.D. degree (with a specialization in microwave and optoelectronics) from the Institut National Polytechnique de Grenoble (INPG), Grenoble, France, in 1990.

He then joined the faculty of electrical engineering as an Associate Professor with the Ecole Nationale Supérieure d'électronique et de Radioélectricité de Grenoble (ENSERG), Grenoble, France, where he teaches microwave techniques and electromagnetic modeling. He is currently a Professor with the Université Joseph Fourier, Grenoble, France, and the Institut Universitaire de Technologie (IUT), Grenoble, France. His research activity with the Institut de Microélectronique d'Electromagnétisme et Photonique (IMEP) focuses on the characterization and electromagnetic modeling of microwave and high-speed circuits, and their integration on silicon/silicon-on-insulator (SOI) technologies.

Kate A. Remley (S'92–M'99) was born in Ann Arbor, MI, in 1959. She received the Ph.D. degree in electrical and computer engineering from Oregon State University, Corvallis, in 1999.

From 1983 to 1992, she was a Broadcast Engineer in Eugene, OR. From 1989 to 1991, she was Chief Engineer of an AM/FM broadcast station. In 1999, she joined the Radio-Frequency Technology Division, National Institute of Standards and Technology (NIST), Boulder, CO, as an Electronics Engineer. Her research activities focus on development of metrology for wireless systems, and characterizing the link between nonlinear circuits and system performance.

Dr. Remley was the recipient of the Department of Commerce Silver Medal and the Automatic RF Techniques Group (ARFTG) Best Paper Award.

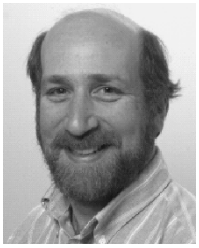

Joel P. Dunsmore (M'83) received the B.S.E.E. and M.S.E.E. degrees from Oregon State University, Corvallis, in 1982 and 1983, respectively.

He is currently a Senior Design Engineer with the Component Test Division, Agilent Technologies (formerly the Hewlett-Packard Company), Santa Rosa, CA. He has also been involved with consulting on measurement applications. He has authored or coauthored numerous papers on measurement technology. He has recently been involved in the research of nonlinear testing including differential devices, and mixer measurements. He holds 14 patents related to his research.

Paul D. Hale (M'01–SM'01) received the Ph.D. degree in applied physics from the Colorado School of Mines, Golden, CO, in 1989.

Since 1989, he has been a Staff Member with the National Institute of Standards and Technology (NIST), Boulder, CO, where he has conducted research in birefringent devices, mode-locked fiber lasers, fiber chromatic dispersion, broad-band lasers, interferometry, polarization standards, and high-speed opto-electronic measurements. He is currently the Leader of the High-Speed Measurements Project of the Sources and Detectors Group. His research interests include high-speed opto-electronic and microwave measurements and their calibration.

Dr. Hale is currently an associate editor of the JOURNAL OF LIGHTWAVE TECHNOLOGY. Along with a team of four scientists, he was the recipient of the 1994 Department of Commerce Gold Medal for measuring fiber cladding diameter with an uncertainty of 30 nm. Along with four other scientists, he was the recipient of a 1998 Department of Commerce Bronze Medal for developing measurement techniques and standards to determine optical polarization parameters.

Jack C. M. Wang received the Ph.D. degree in statistics from Colorado State University, Fort Collins, in 1978.

He is currently a Mathematical Statistician with the Statistical Engineering Division, National Institute of Standards and Technology (NIST), Boulder, CO. His research interests include interval estimation on variance components, statistical graphics and computing, and the application of statistical methods to physical sciences.

Dr. Wang is a Fellow of the American Statistical Association.

Tracy S. Clement (S'89–M'92–SM'05) received the Ph.D. degree in electrical engineering from Rice University, Houston, TX, in 1993. Her doctoral research involved the development and study of a variety of ultrashort pulse and very short wavelength lasers.

Since 1998, she has been with the Optoelectronics Division, National Institute of Standards and Technology (NIST), Boulder, CO. Her current research interests include the development of measurement systems for high-speed electro-optic components, as well as ultrashort pulse laser measurements. Prior to joining the Optoelectronics Division, NIST, she was an Associate Fellow of the JILA, the Quantum Physics Division, NIST, and was an Assistant Professor Adjoint with the Department of Physics, University of Colorado at Boulder. From 1993 to 1995, she was a Director's Post-Doctoral Fellow with Los Alamos National Laboratory, Los Alamos, NM.